Published in final edited form as:
Nat Immunol. 2009 January ; 10(1): 101–108. doi:10.1038/ni.1675.

The Duffy antigen receptor for chemokines transports chemokines and supports their promigratory activity

Monika Pruenster[1], **Liesbeth Mudde**[1], **Paula Bombosi**[1], **Svetla Dimitrova**[1], **Marion Zsak**[1], **Jim Middleton**[1,2], **Ann Richmond**[3], **Gerard J Graham**[4], **Stephan Segerer**[5,6], **Robert J B Nibbs**[4], and **Antal Rot**[1]

[1]Experimental Pathology, Novartis Institutes for BioMedical Research, Vienna A-1230, Austria [2]Medical School, Keele University, Robert Jones & Agnes Hunt Orthopaedic Hospital, Oswestry SY10 7AG, UK [3]Department of Veterans Affairs and Department of Cell Biology, Vanderbilt University School of Medicine, Nashville, Tennessee 37232, USA [4]Division of Immunology, Infection and Inflammation, Glasgow Biomedical Research Centre, University of Glasgow, Glasgow G12 8TA, UK [5]Medizinische Poliklinik, University of Munich, Munich D-80337, Germany [6]Clinic for Nephrology, University of Zurich, Zurich CH-8091, Switzerland

Abstract

The Duffy antigen receptor for chemokines (DARC) belongs to a family of 'silent' heptahelical chemokine receptors that do not couple to G proteins and fail to transmit measurable intracellular signals. DARC binds most inflammatory chemokines and is prominently expressed on venular endothelial cells, where its function has remained contentious. Here we show that DARC, like other silent receptors, internalized chemokines but did not effectively scavenge them. Instead, DARC mediated chemokine transcytosis, which led to apical retention of intact chemokines and more leukocyte migration across monolayers expressing DARC. Mice overexpressing DARC on blood vessel endothelium had enhanced chemokine-induced leukocyte extravasation and contact-hypersensitivity reactions. Thus, interactions of chemokines with DARC support their activity on apposing leukocytes *in vitro* and *in vivo*.

Chemokine-induced egress of leukocytes from the circulation is a fundamental component of inflammation. Similar to directed *in vitro* leukocyte migration, leukocyte egress is induced by chemokine signaling through G protein–coupled receptors[1]. However, *in vitro* chemotaxis does not replicate the intricacies of leukocyte emigration that entails multiple molecular contacts between the adhesion molecules on leukocytes and endothelial cells[2]. In addition, to induce leukocyte emigration, chemokines themselves must engage in complex interactions with endothelial cells. These include the immobilization of chemokines on the luminal surface[3,4] and, for tissue-derived chemokines, their transcytosis from the abluminal

Correspondence should be addressed to A.R. (antal@gmx.net).

Supplementary information is available on the Nature Immunology website.

AUTHOR CONTRIBUTIONS

M.P., L.M. and P.B. designed and did experiments, analyzed data and contributed to the preparation of the manuscript; S.D., M.Z. and J.M. designed and did experiments and analyzed data; A.Ri., G.J.G., S.S. and R.J.B.N. provided critical material and contributed to data analysis; and A.Ro. directed the research, designed experiments, analyzed data and wrote the manuscript.

COMPETING INTERESTS STATEMENT

The authors declare competing financial interests: details accompany the full-text HTML version of the paper at http://www.nature.com/natureimmunology/.

(basal) side to the luminal side of endothelium[4]. Glycosaminoglycans (GAGs), heparan sulfate in particular, avidly bind chemokines[5,6] and are abundant on the luminal endothelial cell surface[6,7]. There, GAGs immobilize chemokines and support their pro-emigratory activities[4,8,9]. Furthermore, *in vitro* chemokine transcytosis is diminished in endothelial cells that lack heparan sulfate[9]. However, several studies have postulated that another molecule, the Duffy antigen receptor for chemokines (DARC), mediates the interactions of chemokines with endothelial cells[4,10–13]. In addition to erythrocytes, venular endothelial cells selectively express DARC[14]. The unique chemokine specificity of DARC, which binds both CC and CXC inflammatory chemokines[15], is identical to the profile of the *in situ* binding of chemokines to venular endothelium in human skin[10]. Because DARC lacks completely the Asp-Arg-Tyr consensus motif in its second cytoplasmic loop, it cannot couple to G proteins and subsequent signaling pathways[16]. On the basis of that feature, DARC is grouped with two other heptahelical molecules, D6 and CCX-CKR, to form a family of atypical 'silent' chemokine receptors[17,18]. Both D6 and CCX-CKR have been shown to act as chemokine 'decoy receptors'; they bind and internalize inflammatory and homeostatic CC chemokines, respectively, and target them into lysosomes for their efficient degradation[19–21]. Consequently, lack of D6 expression *in vivo* results in enhanced chemokine-mediated responses in experimental inflammation and carcinogenesis[22–24]. It has been widely assumed that DARC expressed by endothelial cells may also function as a chemokine 'decoy receptor' mainly by analogy with D6 and CCX-CKR, as well as on the basis of findings showing a 'sink function' for DARC on erythrocytes[25], exaggerated responses to lipopolysaccharide in DARC-deficient mice[26] and diminished chemokine-induced angiogenesis in DARC-transgenic mice[27]. Here we set out to determine unequivocally if DARC expressed by endothelial cells diminishes or sustains chemokine availability and function *in vitro* and *in vivo*. For this, we used DARC-transfected cells to ascertain its function in the binding, internalization, scavenging and transcytosis of cognate chemokines. We studied the contribution of DARC expressed by endothelial cells to leukocyte emigration *in vivo* in DARC-transgenic (mDARCtg) mice, which overexpress DARC on their endothelial cells[27]. Our results show that unlike other known silent chemokine receptors, DARC did not act as a decoy but instead supported chemokine activity and was required for optimal chemokine-induced leukocyte migration *in vitro* and *in vivo*.

RESULTS

Ultrastructural localization of DARC in skin venules

Inflammatory chemokines injected into skin are transported across the endothelium[4]. Immunoelectron microscopy studies have shown that chemokines bind to endothelial cells abluminally, appear in the cytoplasm in plasmalemmal and large electron-lucent vesicles and become immobilized on the luminal endothelial cell membrane[4]. We used this experimental setup to study the ultrastructural localization of DARC in endothelial cells after *ex vivo* injection of cognate chemokine into human skin. DARC immunoreactivity was located together with injected chemokine in venular endothelial cells on the abluminal membrane, in the intracellular plasmalemmal and large electron-lucent vesicles as well as on the luminal cell membrane (Fig. 1). These data suggest that DARC may contribute to the binding, internalization and transport of chemokines by endothelial cells.

Subcellular distribution of DARC in transfected cells

To study the potential function of DARC in chemokine binding and internalization, we turned next to *in vitro* assay systems. Because neither the primary nucleated cells nor the transformed cells available to us expressed DARC (data not shown), we transfected Madin-Darby canine kidney (MDCK) cells with pcDNA3.1 vector encoding DARC (MDCK-DARC cells) or empty vector (MDCK-mock cells). We used MDCK-DARC cells grown on

Transwell filters to investigate the subcellular localization of DARC with and without stimulation by cognate chemokines. As shown by confocal microscopy and immunoelectron microscopy, DARC immunoreactivity was evenly distributed between the apical and basolateral cell surfaces of unstimulated MDCK-DARC cells (Fig. 2a and Supplementary Fig. 1a and Table 1 online). The addition of a cognate chemokine CCL2 to the basolateral side of monolayers resulted in the redistribution of DARC immunoreactivity into the cytoplasm (Fig. 2b and Supplementary Table 1), where it localized together with CCL2 and caveolin in intracellular vesicles (Supplementary Fig. 2a,b online). Over time, DARC accumulated on the apical side of the cells (Fig. 2c and Supplementary Table 1) and was associated mainly with the microvillus membrane extensions (Fig. 2d), where it localized together with CCL2 (Fig. 2e). After a recovery period of 16 h, DARC reappeared on the basal surface (data not shown). The observed chemokine-induced redistribution of DARC from the basolateral membrane through an intracellular vesicular compartment onto the apical membrane is consistent with its putative function in chemokine transcytosis. The following experiments addressed this possibility directly.

DARC-mediated chemokine transport across cell monolayers

We used radioiodinated chemokines to study the influence of DARC expression on their ability to pervade monolayers of MDCK cells grown on Transwell inserts. First, we added ^{125}I-labeled CCL2 below the Transwell filters to the basolateral side of MDCK-DARC cells and, for comparison, monolayers of MDCK-mock cells. After incubation, we measured the radioactivity above the filters in the following distinct compartments: intracellular; immobilized on the apical cell surface; and in the fluid in the top compartment. Furthermore, trichloroacetic acid (TCA) precipitation of these fractions allowed to distinguish between intact chemokines (TCA precipitable) and degraded chemokines (TCA soluble).

The expression of DARC by MDCK cells resulted in significantly more chemokine transcytosis across the monolayers at both early and late time points (Fig. 3a). A substantial portion of the transported chemokine cargo remained associated with the apical membrane of MDCK-DARC cells. Gel autoradiography confirmed that^{125}I-labeled CCL2 in the MDCK-DARC cells and on their apical membrane was the full-length intact chemokine (Fig. 3b). When we applied ^{125}I-labeled CCL2 above the MDCK-DARC monolayers, it bound efficiently onto the apical surface and was internalized in part (Fig. 3c). However, neither the bound chemokine fraction nor the internalized one increased with time. Also, we found no contribution of DARC expression to transport in the apical-to-basolateral direction (Fig. 3d). The ‘architecture’ of the Transwell setup did not influence the direction of chemokine transport. The transport of ^{125}I-labeled CCL2 also took place in the basolateral-to-apical direction but not vice versa when MDCK-DARC monolayers were grown on the bottom side of the filters (data not shown).

The data describing the transport of ^{125}I-labeled CCL2 were closely recapitulated with another DARC ligand, CXCL8 (data not shown). In contrast, a noncognate chemokine, CCL19, did not bind specifically to MDCK-DARC cells and was neither internalized nor transported (Supplementary Fig. 3a online). The simultaneous addition of CCL2 did not induce any change in the uptake or transport of ^{125}I-labeled CCL19 (Supplementary Fig. 3b). These findings support the idea that DARC is directly involved in the process of chemokine transcytosis rather than triggering nonspecific uptake and transport by MDCK-DARC cells.

To evaluate the potential contribution of DARC to chemokine degradation, we measured the TCA-soluble fraction of radioactivity after incubating ^{125}I-labeled CCL2 with MDCK-DARC cells and, for comparison, MDCK cells transfected with D6. When ^{125}I-labeled

CCL2 was placed below the monolayer, only a negligible portion of it was degraded in the process of transcytosis by MDCK-DARC cells (Fig. 4a). Degradation was more apparent when the chemokine was placed above the MDCK-DARC monolayers (Fig. 4b); nevertheless, it remained a small fraction of that obtained with MDCK cells transfected with D6.

We also found DARC-mediated chemokine transport in another nucleated cell type, DARC-transfected immortalized human umbilical vein endothelial cells (HUVEC-DARC). HUVEC-DARC monolayers internalized and transported intact ^{125}I-labeled CCL2 from the basolateral to the apical side and, notably, unlike their mock-transfected counterparts, retained most of the chemokine cargo on their apical surface (Fig. 5a). Chemokine applied to the apical surface of these cells bound readily and a small part of it was internalized (Fig. 5b) but was not transported in basolateral direction (Fig. 5c).

Contribution of DARC to monocyte transmigration

To determine whether the DARC-mediated chemokine transport affected leukocyte transmigration across the monolayers, we used the following Transwell setup. We added either buffer or CCL2 to the bottom wells and, 1 h later, placed monocytes labeled with the cytosolic dye CFSE above the mock- or DARC-transfected monolayers and then allowed the cells to migrate for 4 h. We counted transmigrated monocytes in the following compartments: adherent to the bottom plate, in suspension in the bottom well, and adherent to the bottom side of the filters (Fig. 6). Relative to control, CCL2 induced the transmigration of monocytes across both MDCK-mock and MDCK-DARC monolayers with significantly more monocyte transmigration across MDCK-DARC cells (Fig. 6a). No monocyte transmigration was induced when CCL2 was added above the monolayers regardless of whether the MDCK cells expressed DARC or not (data not shown).

In vivo, in the process of chemokine-induced leukocyte emigration, the flow of blood removes chemokines that are not anchored to the luminal endothelial cell surface[3]. In contrast, in a static *in vitro* Transwell system, nonimmobilized soluble chemokines may also influence leukocyte migration and obscure the contribution of chemokine presentation. To address that issue, in a separate set of experiments we assembled the Transwell systems as described above but repeatedly exchanged the fluid in the upper compartment during the incubation. We did this to remove the soluble CCL2 and to replace nonadherent monocytes, thus mimicking *in vitro,* in admittedly a rather rudimentary way, the conditions of blood flow. This ‘purely manual flow chamber’ (PMFC) allowed us to identify the functional contribution of chemokine immobilization by DARC to leukocyte transmigration. The difference in transmigration across MDCK-DARC cells versus MDCK-mock cells was greater in the PMFC conditions (Fig. 6a). In three independent experiments with cells from different donors in standard Transwell assays, on average 1.6-fold more monocytes migrated across the monolayers expressing DARC, whereas in the PMFC, this difference was on average 4.3-fold (standard deviation, 0.9 and 1.1, respectively).

We also confirmed the consequences of chemokine interactions with DARC for monocyte transmigration using HUVEC-DARC monolayers. The expression of DARC on HUVECs significantly enhanced the transmigration of monocytes (Fig. 6b). Notably, most migrated monocytes remained attached to the bottom side of the Transwell filters. The cells in this compartment would not have been accounted for in a traditional Transwell procedure, in which only the cells in suspension are evaluated.

The enhanced monocyte transmigration across DARC-transfected cells was not due to greater monolayer permeability, which putatively may be induced by either DARC expression or CCL2 signaling. As shown by diffusion of the tracer inulin across the

monolayers as well as by their electrical resistance, the DARC-transfected monolayers were at least as tight as their mock-transfected counterparts in the presence or absence of CCL2 (Supplementary Fig. 4 online). Thus, DARC facilitates leukocyte transmigration across the monolayers expressing it and supports *in vitro* chemokine activity.

Neutrophil emigration in mDARCtg and wild-type mice

Next we compared neutrophil emigration in response to intraperitoneal and intradermal injection of the DARC ligand mouse CXCL1 (also called KC) in wild-type mice and in mDARCtg mice, which (as noted above) overexpress DARC on endothelial cells[27]. We chose this chemokine because it attracts neutrophils that are normally mostly absent from the peritoneal cavity and skin. Intraperitoneal and intradermal injection of CXCL1 resulted in the recruitment of significantly more neutrophils in mDARCtg mice than in their wild-type counterparts (Fig. 7). Thus, overexpression of DARC on endothelial cells leads to enhanced *in vivo* proemigratory activity of chemokines.

Contact hypersensitivity in mDARCtg and wild-type mice

To study the contribution of DARC on endothelial cells to leukocyte emigration in the more complex disease setting of inflammatory pathology, we compared the development of contact hypersensitivity (CHS) in wild-type and mDARCtg mice. We sensitized mice with 2% oxazolone and elicited CHS 1 week later by two applications of 0.2% oxazolone to the ear. We evaluated the CHS reaction by measuring ear thickness and weight, as well as by assessing the histological appearance of the lesions. The CHS lesions of mDARCtg mice were more severe than those of wild-type mice (Fig. 8). The ears of mDARCtg mice were significantly thicker at each time point measured (Fig. 8a). That difference was also reflected by significantly greater ear weights of mDARCtg mice at the termination of the experiment (Fig. 8b) and by the histomorphological appearance of the lesions (Fig. 8c). The dermis of mDARCtg mice was thicker and contained more mononuclear cells, neutrophils and eosinophils. Also, the thickening of the epidermis was more prominent in mDARCtg mice, which reproducibly had many epidermal microabsesses (Fig. 8c). Thus, overexpression of DARC on endothelial cells leads to enhanced leukocyte emigration into the skin lesions of CHS. These findings demonstrate that DARC on endothelial cells has a pro-emigratory function and establish DARC as an auxiliary molecule that supports optimal *in vivo* leukocyte responses to chemokines.

DISCUSSION

DARC belongs to a family of silent heptahelical chemokine receptors that fail to transmit conventional G protein–mediated signals[17,18] but can substantially influence chemokine activity *in vivo*. The silent receptor D6 scavenges chemokines[19,20], and its expression influences the severity of experimental inflammation[22,23] and the efficiency of tumorigenesis[24]. A similar function in chemokine scavenging has been suggested for CCX-CKR[21]. In this study we have identified the opposite end of the spectrum of activities exerted by silent chemokine receptors. We have shown that in complex cell systems, DARC supported the promigratory function of chemokines. When transfected into nucleated cells, DARC acted as a unidirectional transporter of cognate chemokines. In contrast to findings obtained with D6 and CCX-CKR[19–21], we detected only minor degradation of chemokines as a consequence of their interaction with DARC. Accordingly, unlike D6, which localizes into recycling endosomes[20,28], DARC, after being internalized into MDCK cells, was targeted into caveolae. Our *in vitro* data are in agreement with published results[29] and *in vivo* observations of DARC immunoreactivity in endothelial cell caveolae, as well as published findings linking this organelle to chemokine transcytosis[4]. It is possible that silent chemokine receptors contain functional domains responsible for their alternative coupling

with endocytotic or transcytotic pathways. This in turn would determine the fate of their cargo and ultimately the physiological function of an individual silent chemokine receptor. It has been shown that the serine cluster at the carboxyl terminus of D6 determines its constitutive phosphorylation, intracellular 'itinerary' and resistance to desensitization but not the internalization itself[30]. It is not known if DARC contains any specific domains responsible for its internalization, caveolar targeting and transcellular routing. Alternatively, it is also possible that the biochemical makeup of different cells, such as the relative preponderance of transcytotic versus endocytotic 'machineries' or momentarily manifest functional cell programs, determines the route and outcome of chemokine internalization by silent chemokine receptors.

It is important to emphasize that the chemokine-induced internalization of DARC represents a true receptor-mediated cellular response. The molecular effectors involved in this process are not yet apparent and may include β-arrestin, Rab GTPases and several kinases shown to be activated in G protein–coupled receptors independently of G proteins[31,32]. The feature of ligand-triggered receptor internalization sets DARC apart from D6 yet again. The latter is also constitutively internalized in the absence of ligand occupancy[20,28,30]. However, ligation of D6 by chemokines augments its translocation from intracellular stores onto the cell surface[28]. Not only did chemokines induce DARC internalization but also their association with DARC was required for their transcytotic 'itinerary'. The noncognate chemokine CCL19 was neither internalized nor transported by DARC, not even when the transcytotic 'machinery' was triggered by a cognate chemokine.

A distinctive attribute of chemokine transcytosis by DARC was the retention of a substantial portion of the transported chemokine on the apical surface. In fact, the apical membrane–associated chemokine fraction accounted in large part for the difference in chemokine transport in DARC- versus mock-transfected cells. The surface retention of transported chemokines may explain why the direct contribution of DARC to chemokine transcytosis has not been reported before[11]. Analogous to our *in vitro* findings, the process of endothelial cell transcytosis *in vivo* results in immobilization of chemokines on the luminal membrane and its microvillus extensions in particular[4]. Our functional and morphological data collectively suggest that DARC may directly be involved in the retention of chemokines on apical and luminal surfaces. Moreover, we speculate that similar to the function now ascribed exclusively to endothelial GAGs[33], DARC may present chemokines to their receptors on apposing leukocytes. It is noteworthy that we did not detect any contribution of GAGs to chemokine transport or their apical immobilization. CCL19 can bind GAGs[34] but did not associate with MDCK cells and was neither internalized nor transported. Also, treatment with optimal concentrations of heparinase I and III or chondroitinase ABC, or a 'cocktail' of these, failed to remove CCL2 immobilized on the apical surface (data not shown). Of course, these results do not challenge the overall importance of GAGs in chemokine immobilization[6]. It still remains to be established if DARC acts together with GAGs in chemokine transport and presentation or if alternative DARC- and GAG-mediated pathways accomplish these tasks.

DARC expression by the monolayers resulted in superior chemokine-induced leukocyte transmigration across them. This could simply have been an enhanced response to the surplus of chemokines transported by DARC. Furthermore, DARC targeted chemokines into caveolae and onto the apical microvilli, where they could guide the transcellular migration of leukocytes and aid in the adhesion of leukocytes to monolayers, respectively. The latter mechanism has been suggested by a study in which the use of a blocking antibody and silencing by small interfering RNA identified a function for DARC in leukocyte adhesion to endothelium[35].

Our *in vitro* findings showing that DARC sustained chemokine activity were further confirmed *in vivo* with mDARCtg mice[27]. These mice have been used before to investigate the involvement of DARC in chemokine-induced angiogenesis and tumor neovascularisation[27,36]. In contrast to our findings on leukocyte recruitment, overexpression of DARC by endothelial cells results in a diminished angiogenic response[27,36]. These apparently conflicting conclusions may be reconciled by the mechanism of DARC-mediated chemokine transcytosis described here. In fact, chemokines induce angiogenesis and leukocyte emigration by acting at two opposing surfaces of the endothelial cells. Angiogenic budding and sprouting of new vessels take place in response to chemokines present abluminally. Conversely, leukocyte emigration is initiated by chemokines associated with the luminal surface. By transporting chemokines in the abluminal-to-luminal direction, endothelial cell DARC may disrupt the proangiogenic extravascular chemokine patterns and establish luminal pro-emigratory ones. Accordingly, tumors in mDARCtg mice had fewer vessels but more leukocytes than did those in wild-type mice[36]. Alternatively, the suppressed angiogenesis in mDARCtg mice may involve the putative formation of heterodimers of DARC and CXCR2, with consequent silencing of the latter. Although no information exists about the formation of heterodimers by DARC and CXCR2, DARC and CCR5 have been shown to form heterodimers, resulting in the downregulation of CCR5-mediated responses[37].

In addition to using mDARCtg mice, several investigators have used DARC-deficient mice to study the function of DARC in chemokine-mediated pathophysiology. However, such mice lack DARC expression not only on endothelial cells but also on erythrocytes. The suggested many functions of erythroid DARC range from its being a sink[25], scavenging plasma chemokines, to being their reservoir[38], maintaining chemokine plasma concentrations[39]. Plasma chemokines themselves may have diverse leukocyte effects varying from the recruitment of leukocytes from the bone marrow[40,41] to either their priming or their desensitization. Such activities, compounded by the effects of endothelial DARC, have resulted in contradictory reports of phenotypes for DARC-deficient mice[26,42,43].

Many humans of West African ancestry lack erythroid DARC. This is due to a single-nucleotide mutation in the promoter region of the gene encoding DARC that disrupts the binding site for erythroid transcription factor GATA-1 (ref. 44). This explains why these ‘DARC-negative’ people still express DARC on venular endothelial cells[14]. The ‘Duffy-negative’ phenotype has allowed some clinical and epidemiological correlates to be made in terms of the contribution of DARC on erythrocytes to the pathogenesis of human diseases, including malaria[45] and infection with human immunodeficiency virus and AIDS[46]. DARC on erythrocytes has also been suggested to suppress tumor development[47] and dissemination[48]. In contrast, little is known about how DARC on endothelial cells contributes to human disease. The expression of DARC on venules varies among different organs and in tissue sites (unpublished observations). Upregulation of DARC in the venular endothelium and its appearance in segments of the circulatory tree normally devoid of it (arteries, capillaries and large veins) takes place during infection, inflammation and transplant rejection[16,49–52]. Previously, it was not apparent which bias upregulation of DARC may have. Our results suggest that it supports the activity of chemokines and thus contributes to disease pathogenesis.

In conclusion, here we have shown that DARC expressed in nucleated cells transported cognate chemokines and potentiated their promigratory activities on juxtaposed leukocytes. We suggest that DARC expressed on endothelial cells *in vivo* acts in a similar way. There, DARC internalizes and transports tissue-derived inflammatory chemokines onto the luminal endothelial cell surface. That leads to the establishment of functional pro-emigratory

chemokine patterns accessible to the circulating leukocytes. Thus, DARC has an important role in supporting chemokine function that sets it apart from other silent chemokine receptors. We suggest that DARC on endothelial cells may represent a target for therapeutic interventions aimed at simultaneously blocking many inflammatory chemokines.

METHODS

Transfection and stable expression of DARC

MDCK cells were transfected with pcDNA3.1 neomycin vector encoding DARC or D6 or empty vector. Transfected cells were selected by resistance to the aminoglycoside G418. Over 95% of the transfected cells were positive for DARC or D6, as determined by flow cytometry. HUVECs transfected with DARC or empty vector were provided by J.S. Lee and J.S. Rhim.

Cell culture

Transfected MDCK cells were grown in complete Dulbecco's modified Eagle's medium (DMEM) with 10% (vol/vol) FCS, 2 mM L-glutamine, penicillin and streptomycin supplemented with G418 (500 μg/ml). Cells were passaged every 3–4 d when confluent. Transfected HUVECs were cultured in mammary epithelial basal medium with 20% (vol/vol) FCS, 2 mM L-glutamine, penicillin, streptomycin and endothelial cell growth supplement (20 μg/ml; Technoclone) supplemented with hygromycin (100 μg/ml).

Immunoelectron microscopy of *ex vivo* chemokine injection in normal human skin

After informed consent was provided, pieces of normal human skin were obtained from two healthy people undergoing elective reductive plastic surgery as approved by the Shropshire Research and Ethics Committee (UK). Within 1 h of removal, 12 pmol CXCL8 or saline was injected into multiple sites and skin was incubated for 2 h in a 'bath' of RPMI-1640 medium. The injection sites were excised, were fixed for 60 min in 2% (wt/vol) paraformaldehyde and 0.05% (wt/vol) glutaraldehyde in PBS and were processed for immunoelectron microscopy as described[4]. DARC was detected with mouse monoclonal antibody to DARC (anti-DARC; Fy6; CBC-173; a gift from M. Uchikawa) and CXCL8 was detected with rabbit polyclonal anti-CXCL8 (ref. 4; SDS 3E, Novartis Institutes for BioMedical Research). After repeated washes, sections were incubated for 90 min in goat anti–mouse immunoglobulin G (IgG) labeled with 15-nm gold particles and goat anti–rabbit IgG labeled with 5-nm gold particles (RPN 444 and RPN 424, respectively; Amersham). Grids were washed and gold conjugates were enhanced in a silver intensification solution (IntenSE; Amersham), followed by washing in ultrapure water. Sections were counterstained with uranyl acetate and lead citrate and were viewed with a Zeiss EM 10 transmission electron microscope at 80 kV. Control sections were incubated with purified mouse IgG and rabbit immunoglobulin instead of primary antibodies (X0931 and EKO9, respectively; Dako).

Cryoimmunoelectron microscopy of MDCK-DARC monolayers

Cells grown on collagen-coated Falcon Transwell filters (Becton-Dickinson) were fixed overnight at 4 °C in a buffer of 4% (wt/vol) paraformaldehyde and 0.1 M phosphate, pH 7.4. For redistribution and colocalization studies, 35 nM CCL2 (Peprotech) was added to the lower chamber of the Transwell. After 30 min or 2 h of incubation, cells were fixed as described above. After being washed with PBS, samples were cut into 1-mm^2 pieces and were embedded in gelatin. Gelatin blocks were infiltrated overnight at 4 °C with 2.3 M sucrose. Blocks were mounted on pins and were frozen in liquid nitrogen. Ultrathin cryosections of about 60 nm in thickness were cut at –120 °C on an Ultracut UCT ultra-

microtome (Leica) and were transferred to Formvar carbon-coated copper grids (Gröpl). Sections were stained with monoclonal mouse anti–human DARC (Fy6; CBC-173), followed by rabbit anti-mouse (20259; Dako). Finally, sections were incubated for 20 min with protein A conjugated to 15-nm colloidal gold (provided by G. Posthuma). For colocalization studies, polyclonal rabbit anti-CCL2 (RDI-MCP1abrP; RDI) was also used, followed by protein A conjugated to 5-nm colloidal gold. Sections were 'contrasted' by methylcellulose containing 0.6% (wt/vol) uranyl acetate and were examined with an EM 10 transmission electron microscope. Cells stained with mouse IgG and rabbit immunoglobulin (X0931 and EKO9, respectively; Dako) served as controls.

Confocal microscopy of MDCK-DARC monolayers

Cells were grown on collagen-coated Falcon Transwell filters, until confluent, when 35 nM CCL2 (Peprotech) was added to the lower chamber. After 30 or 120 min of incubation, cells were fixed for 5 min in 4% (wt/vol) paraformaldehyde, were washed with PBS and were embedded in optimum cutting temperature compound (Sakura). Cryosections 7 μm in thickness were fixed for 5 min at 21 °C in 4% (wt/vol) paraformaldehyde. After being made permeable for 5 min in 0.5% (vol/vol) Triton X-100 in PBS, sections were incubated for 45 min with monoclonal mouse anti–human DARC. Mouse IgG2b (M-5534; Sigma Aldrich) served as a control. Sections were washed and then were incubated for 30 min with Alexa Fluor 488–conjugated donkey anti-mouse (A21202; Invitrogen). Finally, sections were mounted in Vectashield HardSet mounting medium (Vector Laboratories) and were analyzed with an LSM 5 Pascal confocal microscope (Carl Zeiss). The distribution of immunoreactivity on the apical and basal sides of the monolayers as well as intracellularly was quantified with analySIS software (Soft Imaging Systems). Two sections were prepared from each of the MDCK-DARC monolayers obtained in three independent experiments. Five adjacent completely visible cells per each section were measured separately and values were averaged.

Chemokine binding, transport and degradation and leukocyte migration in the Transwell system

For the preparation of monolayers, transfected MDCK cells and HUVECs were grown on collagen-coated Transwell inserts until they were confluent. For prevention of outgrowth below the filter, medium was added to the bottom plate only 1 d before the assays were done. To ensure that different wells had comparable monolayers, the electrical resistance of the monolayers was measured before all transcytosis and transmigration experiments. In some experiments, the 'tightness' of the monolayers was verified by the addition of the tracer inulin.

For chemokine transcytosis and degradation assays, ^{125}I-labeled CCL2, CXCL8 or CCL19 (0.025 pmol; specific radioactivity, approximately 2,000 Ci/mmol; Perkin Elmer) was added above or below the monolayer (in the top or bottom Transwell chamber), followed by incubation for 3 or 16 h at 37 °C. Then, supernatants were collected from the bottom and top compartments and cell surface–bound chemokine was removed by the addition of 10× PBS for 3 min. This was followed by cell lysis with 0.4% (vol/vol) Triton-X100 to obtain the intracellular radioactivity. TCA precipitation was used to distinguish between the radioactivity associated with intact chemokine (TCA-precipitable fraction) and degraded chemokine (TCA-soluble fraction). The TCA-precipitable fraction was dissolved in 2 M NaOH and 0.05% (wt/vol) SDS. The radioactivity associated with all fractions was measured with a Cobra II gamma counter (Packard). As a control for the influence of the 'architecture' of the Transwell setup, in some experiments cells were grown on the bottom side of the filter and the assay was done as described above.

For gel autoradiography of CCL2 after its transport by MDCK-DARC cells, ^{125}I-labeled CCL2 was applied below MDCK-DARC monolayers grown on Transwell inserts. After 3 h of incubation, the intracellular and apical cell surface–bound TCA-precipitable fractions that could be precipitated by TCA were obtained as described above. Electrophoresis sample buffer (Santa Cruz) containing 0.1 mM EDTA and protease inhibitors (Roche Diagnostics) was added to the samples at a ratio of 1:1. After 30 min of incubation at 37 °C, proteins were separated by electrophoresis through a 16% (wt/vol) tricine gel (Invitrogen). Gels were fixed in a solution of 40% (vol/vol) methanol and 10% (vol/vol) aqueous acetic acid and were shaken for 1 h at 21 °C, then were dried in a gel dryer (Biorad). The ^{125}I-labeled CCL2 was visualized on Hyperfilm (Amersham) developed in an Agfa Curix 60 processor (Bender AG). Native ^{125}I-labeled CCL2 served as a control.

Monocyte migration assays

For these assays, blood was obtained from healthy human donors (who had provided informed consent) as approved by the phlebotomy guidelines of the Novartis Institutes for BioMedical Research. Mononuclear cells were separated by centrifugation on a Ficoll-Hypaque density gradient (Fresenius Kabi). In the next step, monocytes that were at least 95% pure were obtained by immunomagnetic depletion of lymphocytes with a Monocyte Isolation Kit II (Miltenyi Biotech). Transmigration assays were set up as follows. Either buffer alone or 35 nM CCL2 was added to the lower compartments of Transwell systems. After 1 h of equilibration, 5×10^5 monocytes labeled with CFSE (carboxyfluorescein diacetate succinimidyl diester; Invitrogen) were added to each insert and were allowed to migrate across the monolayers for 4 h. Monocytes that had migrated were counted separately in the following compartments: in suspension in the bottom well; adherent to the bottom side of the filter; and adherent to the bottom plate (the last two groups were counted after being removed with 5 nM EDTA). In a separate set of experiments, the medium and the monocyte suspension above the filters were replaced three times after each hour of incubation. After 4 h, transmigrated monocytes were collected from the lower chamber. These PMFC conditions were used to mimic the ‘sink effect’ of blood through the removal of nonimmobilized chemokines. Because the number of input monocytes differed in standard and PMFC conditions, direct comparison of migration to CCL2 was possible only for MDCK-DARC versus MDCK-mock cells but not for standard versus PMFC conditions. However, the DARC-mediated increase in monocyte migration to CCL2 could be compared in standard versus PMFC conditions.

Contribution of DARC to leukocyte emigration *in vivo*

Wild-type mice and mDARCtg mice (expressing DARC under control of the promoter of the gene encoding preproendothelin[27]) were housed in the specific pathogen–free animal facility of the Novartis Institutes for BioMedical Research, Vienna. All animal experimental protocols were approved by the Novartis Institutes for BioMedical Research and municipal animal welfare committees and experiments were done in accordance with the laws of Austria.

For analysis of neutrophil extravasation induced by intradermal injection of chemokine, mouse keratinocyte-derived chemokine (CXCL1; Peprotech) was injected intradermally into mDARCtg and wild-type mice at a dose of 350 pmol per site. Mice were killed 4 h later, then injection sites were excised and were frozen in liquid nitrogen. Samples were transferred into lysing matrix A tubes (MP Biomedicals), were homogenized with the FastPrep-24 sample preparation system (MP Biomedicals) and were sonicated for 20 s on ice. Supernatants were frozen overnight at –80 °C. The number of neutrophils in the tissue samples was determined by measurement of the neutrophil specific myeloperoxidase activity as described[4]. Samples were incubated for 10 min at 37 °C with 3,3′,5,5′-

tetramethylbenzidine (Sigma Aldrich); reactions were stopped by the addition of 4 N sulfuric acid and optical density was measured at 450 nm with a Spectra Max 340pc (Molecular Devices).

For analysis of neutrophil extravasation induced by the intraperitoneal injection of chemokine, mouse CXCL1 was injected into peritoneal cavities of mDARCtg and wild-type mice at a dose of 350 pmol per site. Saline was used as control. Mice were killed after 4 h, peritoneal exudates were collected and the number of peritoneal neutrophils was determined on the basis of absolute and differential cell counts.

CHS reactions

CHS lesions were induced as described[53]. Mice were sensitized with 2% (wt/vol) oxazolone-acetone on the shaved abdomen on day 1. CHS was eliated by 0.02% (wt/vol) oxazolone-acetone was painted onto the inner side of the right ear on days 7 and 9. The left ear was challenged with acetone only and served as a control. CHS was assessed by measurement of ear swelling with a caliper and evaluation of the histological appearance of the lesions according to standard procedures.

Statistical analysis

Student's *t*-test (two-tailed, two-sample unequal variance) was used for all statistical analyses.

Supplementary Material

Refer to Web version on PubMed Central for supplementary material.

Acknowledgments

We thank M. Uchikawa (Japanese Red Cross) for anti-DARC; J.S. Lee (University of Pittsburgh) and J.S. Rhim (Uniformed Services University of the Health Sciences) for HUVECs transfected with DARC or empty vector; G. Posthuma (Utrecht University) for colloidal gold–conjugated protein A; S. Huber for genotyping; and M. Hahn and W. Höllriegl for husbandry. Supported by the European Union Sixth Framework Programme (LSHB-CT-2005-518167 to M.P., L.M., P.B., G.J.G. and A.Ro.), Deutsche Forschungsgemeinschaft (SE 888/4-1 to S.S.) and the Else-Kröner Fresenius Stiftung (to S.S.).

References

1. Rot A, von Andrian UH. Chemokines in innate and adaptive host defense: basic chemokinese grammar for immune cells. Annu Rev Immunol. 2004; 22:891–928. [PubMed: 15032599]
2. Ley K, Laudanna C, Cybulsky MI, Nourshargh S. Getting to the site of inflammation: the leukocyte adhesion cascade updated. Nat Rev Immunol. 2007; 7:678–689. [PubMed: 17717539]
3. Rot A. Endothelial cell binding of NAP-1/IL-8: role in neutrophil emigration. Immunol Today. 1992; 13:291–294. [PubMed: 1510812]
4. Middleton J, et al. Transcytosis and surface presentation of IL-8 by venular endothelial cells. Cell. 1997; 91:385–395. [PubMed: 9363947]
5. Webb LM, Ehrengruber MU, Clark-Lewis I, Baggiolini M, Rot A. Binding to heparan sulfate or heparin enhances neutrophil responses to interleukin 8. Proc Natl Acad Sci USA. 1993; 90:7158–7162. [PubMed: 8346230]
6. Parish CR. The role of heparan sulphate in inflammation. Nat Rev Immunol. 2006; 6:633–643. [PubMed: 16917509]
7. Tanaka Y, Adams DH, Shaw S. Proteoglycans on endothelial cells present adhesion-inducing cytokines to leukocytes. Immunol Today. 1993; 14:111–115. [PubMed: 8466625]

8. Proudfoot AE, et al. Glycosaminoglycan binding and oligomerization are essential for the in vivo activity of certain chemokines. Proc Natl Acad Sci USA. 2003; 100:1885–1890. [PubMed: 12571364]

9. Wang L, Fuster M, Sriramarao P, Esko JD. Endothelial heparan sulfate deficiency impairs L-selectin- and chemokine-mediated neutrophil trafficking during inflammatory responses. Nat Immunol. 2005; 6:902–910. [PubMed: 16056228]

10. Hub E, Rot A. Binding of RANTES, MCP-1, MCP-3, and MIP-1α to cells in human skin. Am J Pathol. 1998; 152:749–757. [PubMed: 9502417]

11. Lee JS, et al. Duffy antigen facilitates movement of chemokine across the endothelium in vitro and promotes neutrophil transmigration in vitro and in vivo. J Immunol. 2003; 170:5244–5251. [PubMed: 12734373]

12. Rot A. Contribution of Duffy antigen to chemokine function. Cytokine Growth Factor Rev. 2005; 16:687–694. [PubMed: 16054417]

13. Pruenster M, Rot A. Throwing light on DARC. Biochem Soc Trans. 2006; 34:1005–1008. [PubMed: 17073738]

14. Peiper SC, et al. The Duffy antigen/receptor for chemokines (DARC) is expressed in endothelial cells of Duffy negative individuals who lack the erythrocyte receptor. J Exp Med. 1995; 181:1311–1317. [PubMed: 7699323]

15. Gardner L, Patterson AM, Ashton BA, Stone MA, Middleton J. The human Duffy antigen binds selected inflammatory but not homeostatic chemokines. Biochem Biophys Res Commun. 2004; 321:306–312. [PubMed: 15358176]

16. Hadley TJ, Peiper SC. From malaria to chemokine receptor: the emerging physiologic role of the Duffy blood group antigen. Blood. 1997; 89:3077–3091. [PubMed: 9129009]

17. Nibbs R, Graham G, Rot A. Chemokines on the move: control by the chemokine “interceptors” Duffy blood group antigen and D6. Semin Immunol. 2003; 15:287–294. [PubMed: 15001178]

18. Mantovani A, Bonecchi R, Locati M. Tuning inflammation and immunity by chemokine sequestration: decoys and more. Nat Rev Immunol. 2006; 6:907–918. [PubMed: 17124512]

19. Fra AM, et al. Cutting edge: scavenging of inflammatory CC chemokines by the promiscuous putatively silent chemokine receptor D6. J Immunol. 2003; 170:2279–2282. [PubMed: 12594248]

20. Weber M, et al. The chemokine receptor D6 constitutively traffics to and from the cell surface to internalize and degrade chemokines. Mol Biol Cell. 2004; 15:2492–2508. [PubMed: 15004236]

21. Comerford I, Milasta S, Morrow V, Milligan G, Nibbs R. The chemokine receptor CCX–CKR mediates effective scavenging of CCL19 in vitro. Eur J Immunol. 2006; 36:1904–1916. [PubMed: 16791897]

22. Jamieson T, et al. The chemokine receptor D6 limits the inflammatory response *in vivo*. Nat Immunol. 2005; 6:403–411. [PubMed: 15750596]

23. Martinez de la Torre Y, et al. Protection against inflammation- and autoantibody-caused fetal loss by the chemokine decoy receptor D6. Proc Natl Acad Sci USA. 2007; 104:2319–2324. [PubMed: 17283337]

24. Nibbs RJ, et al. The atypical chemokine receptor D6 suppresses the development of chemically induced skin tumors. J Clin Invest. 2007; 117:1884–1892. [PubMed: 17607362]

25. Darbonne WC, et al. Red blood cells are a sink for interleukin 8, a leukocyte chemotaxin. J Clin Invest. 1991; 88:1362–1369. [PubMed: 1918386]

26. Dawson TC, et al. Exaggerated response to endotoxin in mice lacking the Duffy antigen/receptor for chemokines (DARC). Blood. 2000; 96:1681–1684. [PubMed: 10961863]

27. Du J, et al. Potential role for Duffy antigen chemokine-binding protein in angiogenesis and maintenance of homeostasis in response to stress. J Leukoc Biol. 2002; 71:141–153. [PubMed: 11781390]

28. Bonecchi R, et al. Regulation of D6 chemokine scavenging activity by ligand- and Rab11-dependent surface up-regulation. Blood. 2008; 112:493–503. [PubMed: 18480427]

29. Chaudhuri A, et al. Detection of Duffy antigen in the plasma membranes and caveolae of vascular endothelial and epithelial cells of nonerythroid organs. Blood. 1997; 89:701–712. [PubMed: 9002974]

30. McCulloch CV, et al. Multiple roles for the C-terminal tail of the chemokine scavenger D6. J Biol Chem. 2008; 283:7972–7982. [PubMed: 18201974]
31. Drake MT, Shenoy SK, Lefkowitz RJ. Trafficking of G protein-coupled receptors. Circ Res. 2006; 99:570–582. [PubMed: 16973913]
32. Brzostowski JA, Kimmel AR. Signaling at zero G: G-protein-independent functions for 7-TM receptors. Trends Biochem Sci. 2001; 26:291–297. [PubMed: 11343921]
33. Handel TM, Johnson Z, Crown SE, Lau EK, Proudfoot AE. Regulation of protein function by glycosaminoglycans–as exemplified by chemokines. Annu Rev Biochem. 2005; 74:385–410. [PubMed: 15952892]
34. Christopherson KW, Campbell JJ, Travers JB, Hromas RA. Low-molecular-weight heparins inhibit CCL21-induced T cell adhesion and migration. J Pharmacol Exp Ther. 2002; 302:290–295. [PubMed: 12065729]
35. Smith E, et al. Duffy antigen receptor for chemokines and CXCL5 are essential for the recruitment of neutrophils in a multicellular model of rheumatoid arthritis synovium. Arthritis Rheum. 2008; 58:1968–1973. [PubMed: 18576313]
36. Horton LW, Yu Y, Zaja-Milatovic S, Strieter RM, Richmond A. Opposing roles of murine duffy antigen receptor for chemokine and murine CXC chemokine receptor-2 receptors in murine melanoma tumor growth. Cancer Res. 2007; 67:9791–9799. [PubMed: 17942909]
37. Chakera A, Seeber RM, John AE, Eidne KA, Greaves DR. The duffy antigen/receptor for chemokines exists in an oligomeric form in living cells and functionally antagonizes CCR5 signaling through hetero-oligomerization. Mol Pharmacol. 2008; 73:1362–1370. [PubMed: 18230715]
38. Fukuma N, et al. A role of the Duffy antigen for the maintenance of plasma chemokine concentrations. Biochem Biophys Res Commun. 2003; 303:137–139. [PubMed: 12646177]
39. Jilma-Stohlawetz P, et al. Fy phenotype and gender determine plasma levels of monocyte chemotactic protein. Transfusion. 2001; 41:378–381. [PubMed: 11274594]
40. Palframan RT, Collins PD, Williams TJ, Rankin SM. Eotaxin induces a rapid release of eosinophils and their progenitors from the bone marrow. Blood. 1998; 91:2240–2248. [PubMed: 9516121]
41. Serbina NV, Pamer EG. Monocyte emigration from bone marrow during bacterial infection requires signals mediated by chemokine receptor CCR2. Nat Immunol. 2006; 7:311–317. [PubMed: 16462739]
42. Kashiwazaki M, et al. A high endothelial venule-expressing promiscuous chemokine receptor DARC can bind inflammatory, but not lymphoid, chemokines and is dispensable for lymphocyte homing under physiological conditions. Int Immunol. 2003; 15:1219–1227. [PubMed: 13679391]
43. Lee JS, et al. The Duffy antigen modifies systemic and local tissue chemokine responses following lipopolysaccharide stimulation. J Immunol. 2006; 177:8086–8094. [PubMed: 17114483]
44. Tournamille C, Colin Y, Cartron JP, Le Van KC. Disruption of a GATA motif in the Duffy gene promoter abolishes erythroid gene expression in Duffy-negative individuals. Nat Genet. 1995; 10:224–228. [PubMed: 7663520]
45. Horuk R, et al. A receptor for the malarial parasite *Plasmodium vivax*: the erythrocyte chemokine receptor. Science. 1993; 261:1182–1184. [PubMed: 7689250]
46. He W, et al. Duffy antigen receptor for chemokines mediates trans-infection of HIV-1 from red blood cells to target cells and affects HIV-AIDS susceptibility. Cell Host Microbe. 2008; 4:52–62. [PubMed: 18621010]
47. Bandyopadhyay S, et al. Interaction of KAI1 on tumor cells with DARC on vascular endothelium leads to metastasis suppression. Nat Med. 2006; 12:933–938. [PubMed: 16862154]
48. Lentsch AB. The Duffy antigen/receptor for chemokines (DARC) and prostate cancer. A role as clear as black and white? FASEB J. 2002; 16:1093–1095. [PubMed: 12087071]
49. Segerer S, et al. The Duffy antigen receptor for chemokines is up-regulated during acute renal transplant rejection and crescentic glomerulonephritis. Kidney Int. 2000; 58:1546–1556. [PubMed: 11012889]
50. Lee JS, et al. Enhanced expression of Duffy antigen in the lungs during suppurative pneumonia. J Histochem Cytochem. 2003; 51:159–166. [PubMed: 12533524]

51. Bruhl H, et al. Expression of DARC, CXCR3 and CCR5 in giant cell arteritis. Rheumatology (Oxford). 2005; 44:309–313. [PubMed: 15572394]

52. Gardner L, et al. Temporal expression pattern of Duffy antigen in rheumatoid arthritis: up-regulation in early disease. Arthritis Rheum. 2006; 54:2022–2026. [PubMed: 16732566]

53. Schneider MA, Meingassner JG, Lipp M, Moore HD, Rot A. CCR7 is required for the in vivo function of $CD4^{+}CD25^{+}$ regulatory T cells. J Exp Med. 2007; 204:735–745. [PubMed: 17371928]

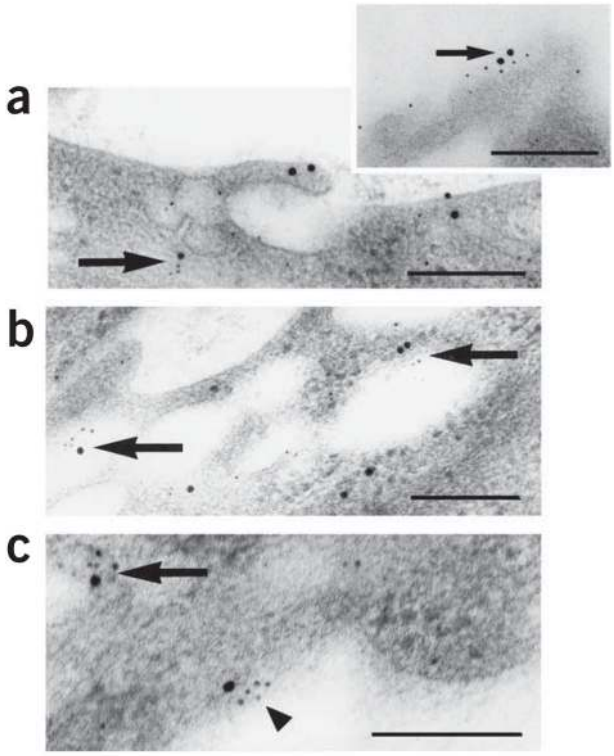

Figure 1.
Colocalization of DARC and CXCL8 in venular endothelial cells in human skin.
Ultrastructural colocalization of DARC immunoreactivity (large black dots; silver-enhanced 15-nm colloidal gold) with CXCL8 immunoreactivity (small black dots; silver-enhanced 5-nm colloidal gold) in plasmalemmal vesicles (**a**) and on the luminal membrane (inset, **a**), in large intracellular electron-lucent vesicles (**b**) and on the abluminal membrane (**c**) in venular endothelial cells 120 min after the injection of CXCL8 (12 pmol) into intact pieces of normal human skin immediately after removal during elective surgery. Large arrows, small arrow and arrowhead indicate colocalization intracellularly, luminally and abluminally, respectively. Scale bars, 200 nm. Results are representative of two experiments with skin samples from two people.

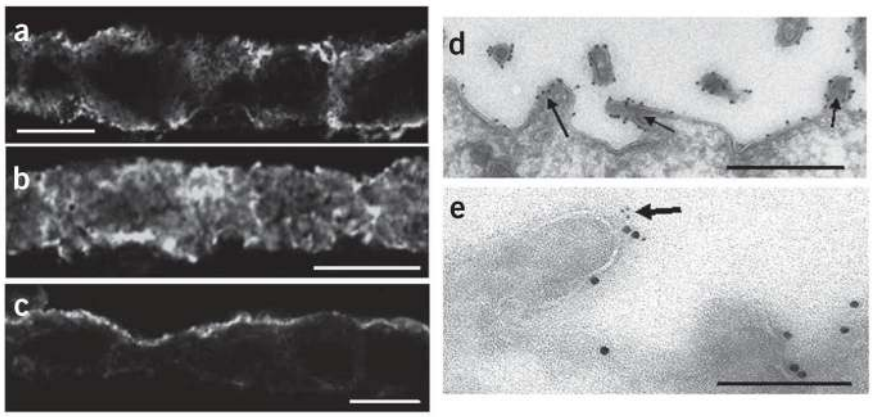

Figure 2.

DARC immunoreactivity in MDCK-DARC monolayers. (**a**–**c**) Confocal laser-scanning microscopy of the subcellular distribution of DARC immunoreactivity in cross-sections of unstimulated (**a**) and CCL2-stimulated (**b**,**c**) MDCK-DARC monolayers grown on Transwell inserts; in **b**,**c**, 35 nM CCL2 was added below the monolayers, followed by incubation for 30 min (**b**) or 2 h (**c**). DARC immunoreactivity was detected by indirect immunofluorescence with Alexa Fluor 488 (quantification of DARC distribution, Supplementary Table 1). Scale bars, 10 μm. (**d**) Immunoelectron microscopy of DARC immunoreactivity (electron-dense dots of colloidal gold) on apical microvillus extensions of MDCK-DARC cells 2 h after the application of CCL2 to the basolateral side. Arrows indicate apical microvilli. Scale bar, 500 nm. (**e**) Immunoelectron microscopy of the colocalization of DARC (large black dots; 15-nm colloidal gold) with CCL2 (small black dots; 5-nm colloidal gold) on an apical microvillus extension (arrow). Scale bar, 200 nm. Images in **d**,**e** were acquired with a transmission electron microscope. Results are representative of at least three independent experiments.

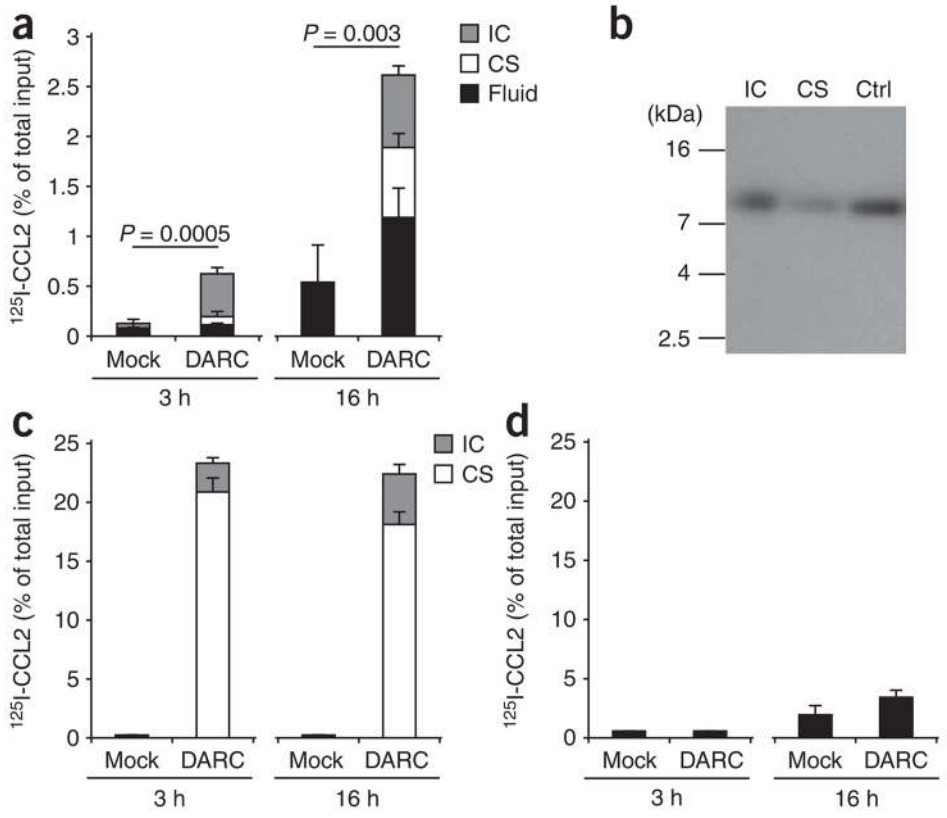

Figure 3.

Chemokine transport by DARC across MDCK-DARC monolayers. Analysis of ^{125}I-labeled CCL2 (^{125}I-CCL2) placed above or below monolayers of MDCK-mock cells (Mock) and MDCK-DARC cells (DARC) and, after incubation, detected in three different compartments: intracellular (IC), cell surface bound (CS) and in the fluid (Fluid). (**a**) Basolateral-to-apical transport of intact ^{125}I-labeled CCL2 TCA-precipitable. (**b**) Autoradiography of MDCK-DARC cell–associated ^{125}I-labeled CCL2 after its basolateral-to-apical transport. Ctrl, native ^{125}I-labeled CCL2 (control). kDa, molecular size in kilodaltons. (**c**,**d**) Binding and internalization (**c**) and transport (**d**) of intact ^{125}I-labeled CCL2 from the apical side to the basolateral side. (**d**) Soluble chemokine in the bottom Transwell chamber. Data are representative of three (**a**,**c**,**d**) or two (**b**) independent experiments (mean and s.d. of three samples).

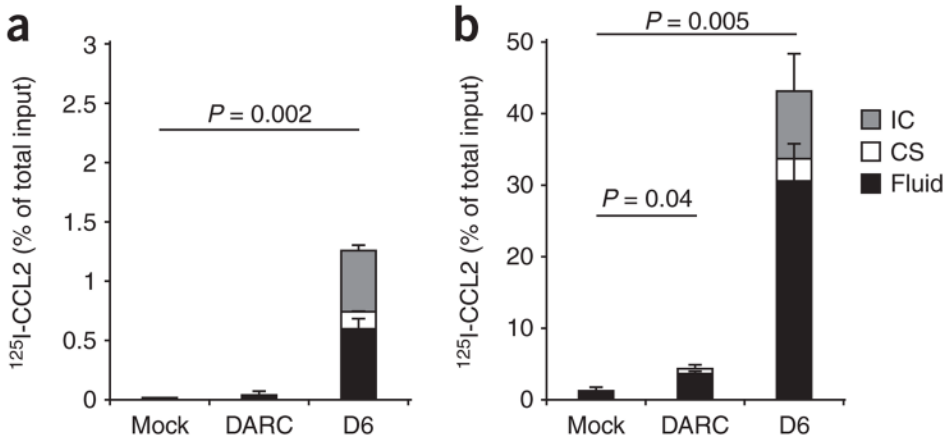

Figure 4.

Chemokine degradation by MDCK cells expressing DARC or D6. Degradation of ^{125}I-labeled CCL2 (detected as the TCA-soluble fraction) by monolayers of MDCK-mock cells, MDCK-DARC cells and MDCK cells transfected with D6 (D6), assessed 3 h after placement below (**a**) or above (**b**) the monolayers. Data are representative of three independent experiments (mean and s.d. of three samples).

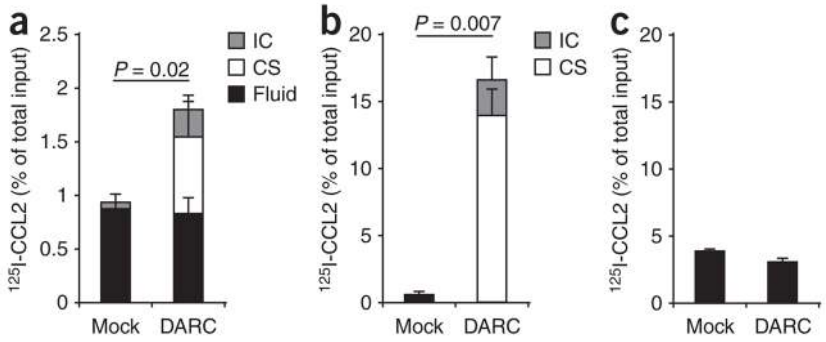

Figure 5.

Chemokine transport by DARC across HUVEC-DARC monolayers. (**a**) Basolateral-to-apical transport of ^{125}I-labeled CCL2 across monolayers of HUVECs transfected with empty vector (Mock) or DARC (DARC) and seeded onto Transwell inserts, assessed after 3 h of incubation. (**b**,**c**) Binding and internalization (**b**) and transport (**c**) of chemokine placed above monolayers of HUVECs transfected with empty vector or DARC. (**c**) Soluble chemokine in the bottom Transwell chamber. Data are representative of two independent experiments (mean and s.d. of three samples).

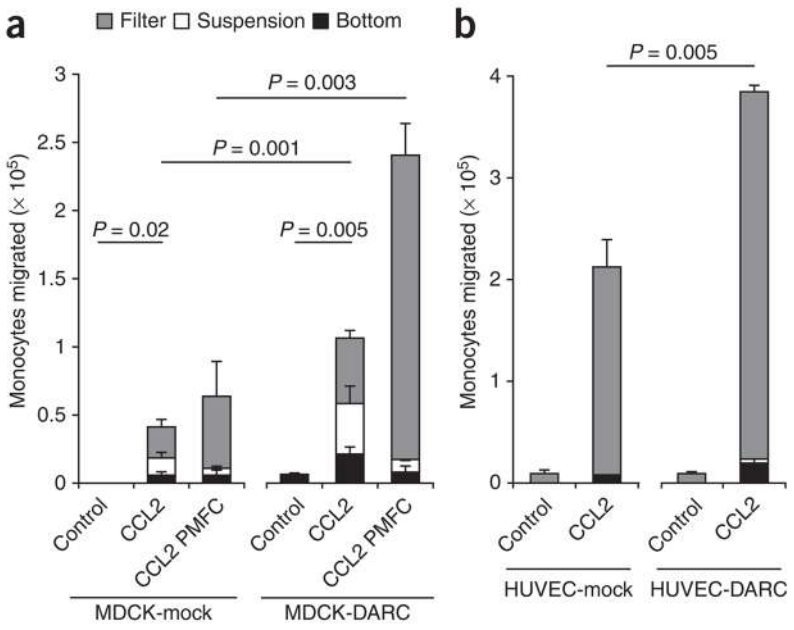

Figure 6.

CCL2-induced monocyte migration across MDCK cells and HUVECs. Migration of human monocytes (isolated from healthy donors) across monolayers of DARC- and mock-transfected MDCK cells (**a**) and HUVECs (**b**) seeded onto Transwell inserts; after 4 h of incubation with 35 nM CCL2, transmigrated monocytes were counted in three different compartments: adherent to the bottom side of the filter (Filter), in suspension in the lower chamber (Suspension) and adherent to the bottom of the chamber (Bottom). (**a**) CCL2 PMFC, replacement of fluid in the upper chamber three times during incubation. Data are representative of three (**a**) or two (**b**) independent experiments (mean and s.d. of three samples).

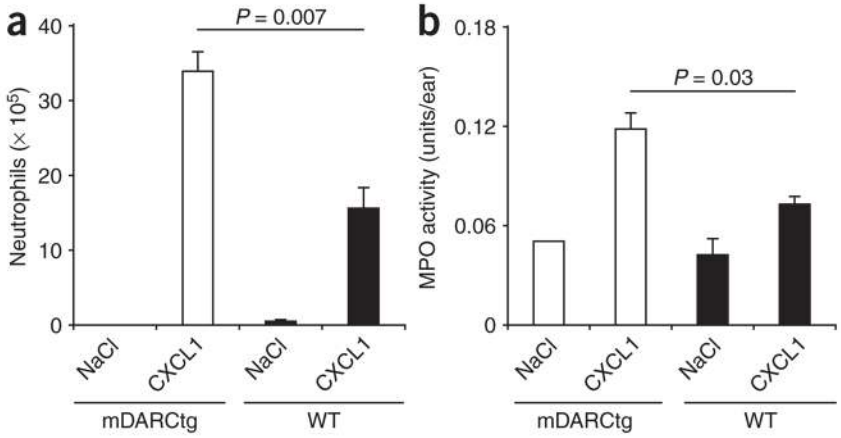

Figure 7.

Recruitment of neutrophils into chemokine injection sites in mDARCtg and wild-type mice. (**a**) Peritoneal neutrophils 4 h after intraperitoneal injection of saline (NaCl; control) or mouse CXCL1 (350 pmol per site) into mDARCtg mice and wild-type (WT) mice ($n = 4$). (**b**) Dermal neutrophil infiltration 4 h after intradermal injection of saline or mouse CXCL1 (350 pmol per site) into mDARCtg and wild-type mice ($n = 4$), assessed as myeloperoxidase (MPO) activity associated with dermal injection sites. Activity in untreated skin biopsies, 0.03 ± 0.01 units per biopsy. Data are representative of three (**a**) or two (**b**) independent experiments (mean and s.e.m.).

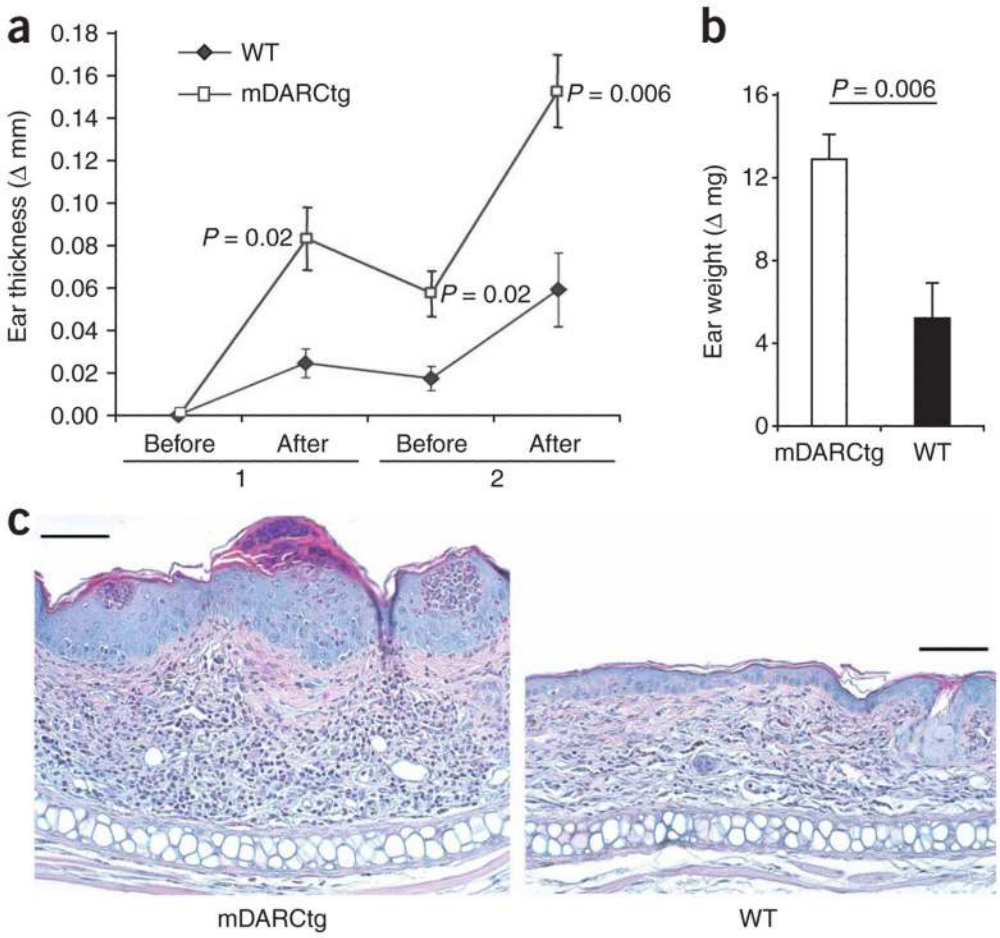

Figure 8.

Acute CHS reaction to oxazolone in mDARCtg and wild-type mice. (**a**) Ear thickness of mDARCtg mice ($n = 5$) and wild-type mice ($n = 8$) sensitized with 2% oxazolone on the shaved abdomen and challenged with 0.2% oxazolone on the ear, measured before and after two challenges (1 and 2) and presented as the difference (Δ mm) between the unchallenged ear and the oxazolone-challenged ear. (**b**) Ear weight after the second oxazolone challenge in **a**, presented as the difference (Δ mg) between the unchallenged ear and the oxazolone-challenged ear. (**c**) Histology of CHS lesions in mDARCtg and wild-type mice. Scale bars, 100 μm. Data are from one of two independent experiments (error bars (**a**,**b**), s.e.m.).